UDC 539.37

I. V. Orynyak, K. A. Kulyk✉, R. V. Mazuryk

3D ANALYSIS OF THE GEOMETRICALLY NONLINEAR DEFORMATION OF BEAMS BY THE METHOD OF BASIC HELICAL ELEMENTS

A general technique is developed for solving the geometrically nonlinear 3D problems on the beams deformation using the helix-form basic solution. The main parameters and features of the "small" helix elements are analyzed and a technique for their iterative alignment into the large 3D structures is thoroughly investigated. It is shown that the basic solution is self-consistent and can be only applied for the analysis of simple geometries, e.g., cantilever beams. The case studies known from the relevant literature are considered, i.e.: a) Bathe's problem for an initially-plane curved beam loaded in the vertical direction; b) Ibrahimbegovich's problem for an initially straight beam loaded by vertical bending moment and axial force; c) Love's problem on the creation of a helix from initially straight flexible beam by applying the end force and moment.

Key words: *deformation, 3D flexible beam, geometric nonlinearity, helix, transfer matrix method, method of basic and corrective solutions.*

Introduction. Beam theories conventionally model the response of thin rods and are widely used in many applications, e.g., civil [8], mechanical [5], and biomedical [16] engineering along with robotics [15, 24] and computer graphics [4, 23]. Despite the apparent simplicity of the physical relationships between the internal forces and deformation in a beam, their analysis remains topical. The problem lies in the geometrically nonlinear behavior, while the theory and techniques for beams operate small displacements associated with the initial (or acquired) geometry. Thus, the main challenge is the numerical realization implying the correctness of the iterative process with the control of geometric transformation.

Theoretical solutions for two-dimensional (planar) cases have a long development history [9]. They are limited to a simple cantilever geometry and have, at best, an educational value. The relevant numerical schemes are still widely studied for specific case studies, finite deformation, material behavior, and application areas [12]. The analysis of a spatially curved rod is much more complicated than the plane one [22]. Theoretical solutions are less detailed and are usually limited to obtaining a helix from an initial straight flexible cantilever beam by applying the concentrated force and moment to its free end. This problem is known as Kirchhoff's problem. It was first solved by Love for an isotropic cross-section of a beam [13] and later considered for beams with different cross-section properties [17].

The most typical numerical approaches imply replacing rod segments (with initial and/or acquired curvature and torsion) with a set of straight sections supplemented by the rotation matrices placed between them [22]. The deformation and displacement of each element are considered in the local orthogonal coordinate system, where the tangential vector is directed along the segment at all stages of the strain computation, which is known as the co-rotational formulation [6]. A weakness of this formulation is the possible bias of the mechanical stress measurements, which leads to an angular shift between straight segments [7].

The recent progress in 3D analysis of geometrically nonlinear beams (GNB) is associated with the use of isogeometric analysis in element formulations, where inhomogeneous rational [10] or cubic [11] B-splines are used as shape functions. The isogeometric analysis allows for the creation of a precise model of continuous geometry. Its advantages are the high analysis accuracy

✉ kostya.kulik@gmail.com

and fast convergence. On the other hand, the integration efficiency is low and the formation of boundary conditions is rather complicated. The vast majority of papers on the 3D analysis of GNB consider relatively simple cases of the cantilever beam deformation. For these statically determined problems, much simpler methods can be applied, e.g., the multiple shooting method, in which the geometry can be calculated by "moving" from the clamped end to the free end [21]. However, the latter method is insufficient for branched and bounded geometries [18].

An efficient technique for formulating boundary conditions for branched structures was developed in [19, 20] based on the basic solutions (BS) and auxiliary (smoothing) solutions (SS). BS takes into account the largest part of the GNB deformation, i.e., its bending and elongation, by representing each element as a segment of a circle, the radius and length of which are derived taking into account the "mounted" internal axial force and bending moment. In addition, the BS geometry establishes a local curvilinear system according to which SS is calculated. It is designed to ensure the perfect geometric and equilibrium continuity between the elements.

Herein, we construct BS for the 3D analysis of GNB based on a helix with geometric characteristics depending on the "mounted" basic moments. In addition to the theoretical substantiation, some numerical examples for the simple case of a cantilever beam are addressed to demonstrate that BS can be regarded as a self-consistent solution that can solve complex modeling problems for GNB.

1. Formulation of the problem within the framework of the method of initial parameters. Consider a C^3-smooth curve that is defined parametrically using radius-vector $\mathbf{p}(s)$, $0 \le s \le \ell$. Introduce tangential vector $\mathbf{t}(s) = \mathbf{p}'(s)$, normal vector $\mathbf{n}(s) = K^{-1}(s)\mathbf{t}'(s)$, and binormal vector $\boldsymbol{\beta}(s) = \mathbf{t}(s) \times \mathbf{n}(s)$, where $K(s) = \|\mathbf{t}'(s)\|$ is the curvature parameter and "$\times$" is the vector product. The introduced vectors form the right-handed triplet, which is known as the Frenet trihedron. Parameter $T(s) = \boldsymbol{\beta}'(s) \cdot \mathbf{n}(s)$, where "$\cdot$" stands for the scalar product, is called a twist.

Making use of the transfer matrix method (TMM) implies consideration of the curve $\mathbf{p}(s)$ as a set of elements $\mathbf{p}_i(s)$, $0 \le s \le \ell_i$, small enough for neglecting the nonlinearity on each of them that is sufficient for formulating the constitutive equations. The conditions of smoothness imply the elements to be coupled and have co-directed tangents and normals, i.e.:

$$\mathbf{p}_i(\ell_i) = \mathbf{p}_{i+1}(0), \quad \mathbf{t}_i(\ell_i) = \mathbf{t}_{i+1}(0), \quad \mathbf{n}_i(\ell_i) = \mathbf{n}_{i+1}(0). \tag{1}$$

The key feature of TMM is the use of an analytical matrix ensuring the connection between the parameters at the beginning of a certain element $s = 0$ and its arbitrary point s. This implies the analytical relationship verbalized by the following connection equations:

$$\mathbf{Y}(s) = \mathbf{A}(s)\mathbf{Y}_0 + \mathbf{B}(s), \tag{2}$$

where $\mathbf{Y}(s)$ is the column-vector of unknown parameters, $\mathbf{Y}_0 = \mathbf{Y}(0)$ is initial state column-vector, $\mathbf{B}(s)$ is the column-vector of free terms involving external loadings and the situation with an element on the previous stage, and $\mathbf{A}(s)$ is the transition matrix [1].

In contrast to the classical routine of TMM, we use a helix instead of a linear segment. Thus, the entire curve $\mathbf{p}(s)$ is approximated with a set of helixes. Each of the helixes is described by the following numerical parameters:

$$p_{0x}, \quad p_{0y}, \quad p_{0z}, \quad t_{0x}, \quad t_{0y}, \quad t_{0z},$$

$$n_{0x},\ n_{0y},\ n_{0z},\quad \beta_{0x},\ \beta_{0y},\ \beta_{0z},\ K, T, \tag{3}$$

where the components with bottom indices $x, y,$ and z indicate the Cartesian coordinates of the corresponding vectors.

Due to the fact that vector $\boldsymbol{\beta}(s)$ is expressed through $\mathbf{t}(s)$ and $\mathbf{n}(s)$, it can be omitted. However, we keep it for the sake of simplicity.

Let us introduce the following parameters:

$$\varphi = s\sqrt{K^2 + T^2}, \quad a = \frac{K}{K^2 + T^2}, \quad h = \frac{T}{K^2 + T^2}. \tag{4}$$

According to the helix geometry [1], we have the displacement vector

$$\mathbf{AB}_p(s) \equiv \left(\frac{h^2\varphi + a^2 \sin\varphi}{\sqrt{a^2 + h^2}},\ a(1 - \cos\varphi),\ \frac{ah(\varphi - \sin\varphi)}{\sqrt{a^2 + h^2}} \right)$$

and the basis rotation matrix

$$\mathbf{AB}_{t,n,\beta}(s) \equiv \begin{pmatrix} \dfrac{h^2 + a^2\cos\varphi}{a^2 + h^2} & \dfrac{a\sin\varphi}{\sqrt{a^2 + h^2}} & \dfrac{ah(1 - \cos\varphi)}{a^2 + h^2} \\ -\dfrac{a\sin\varphi}{\sqrt{a^2 + h^2}} & \cos\varphi & \dfrac{h\sin\varphi}{\sqrt{a^2 + h^2}} \\ \dfrac{ah(1 - \cos\varphi)}{a^2 + h^2} & -\dfrac{h\sin\varphi}{\sqrt{a^2 + h^2}} & \dfrac{a^2 + h^2\cos\varphi}{a^2 + h^2} \end{pmatrix}.$$

Within the context of the latter formulas, the connection equations take the following form:

$$\mathbf{p}(s) = \mathbf{p}_0 + \mathbf{AB}_p(s) \begin{pmatrix} \mathbf{t}_0 \\ \mathbf{n}_0 \\ \boldsymbol{\beta}_0 \end{pmatrix}, \qquad \begin{pmatrix} \mathbf{t}(s) \\ \mathbf{n}(s) \\ \boldsymbol{\beta}(s) \end{pmatrix} = \mathbf{AB}_{t,n,\beta}(s) \begin{pmatrix} \mathbf{t}_0 \\ \mathbf{n}_0 \\ \boldsymbol{\beta}_0 \end{pmatrix}. \tag{5}$$

In such a manner, we have a set of parameters (3), connection equations (5) in the standard form (2), and the trivial conjugation equations (1) sufficient for the realization of the TMM routine.

2. Theoretical substantiation and the solution algorithm.

2.1. Reactions to the applied moments. Let an initially rectilinear element ($K = T = 0$) undergoes the action of an external force $\mathbf{F}$ applied at the point $\mathbf{F}_p$ at a distance $\mathbf{r} = \mathbf{F}_p - \mathbf{p}_0$ from its beginning $\mathbf{p}_0$. This induces the moment $\mathbf{M}_F = \mathbf{r} \times \mathbf{F}$ (Fig. 1). Assume both the point of force application and the force itself to belong to the plane that is formed by the tangential and normal vectors of the element. This produces an angle of deformation:

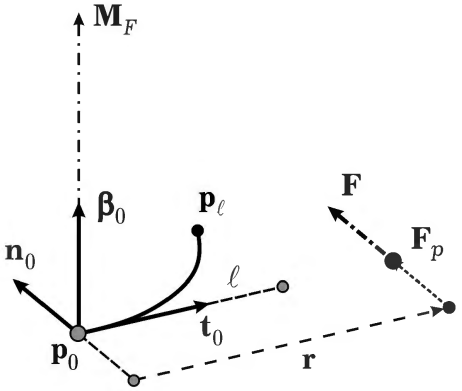

Fig. 1. Action of a complanar force.

$$\Delta\boldsymbol{\theta} = \frac{\mathbf{M}_F}{\mathrm{EI}} \Delta s,$$

where EI is a physical constant. Introduce the vector curvature

$$\mathbf{K} \equiv \frac{\Delta\boldsymbol{\theta}}{\Delta s} = \frac{\mathbf{M}_F}{\mathrm{EI}}.$$

It can be easily shown that the scalar curvature $K = \|\mathbf{K}\|$.

Now, in order to encounter the deformation into an element, we have to make sure its scalar curvature to equal K and rotate the basis so its normal is directed towards the center of the circular segment, i.e.: $\mathbf{n}_0 \perp \mathbf{K}$ and $\boldsymbol{\beta}_0 \parallel \mathbf{K}$. The binormal and normal are then defined as:

$$\boldsymbol{\beta}_0 = \mathbf{K} / \mathrm{K}, \quad \mathbf{n}_0 = \boldsymbol{\beta}_0 \times \mathbf{t}_0 . \tag{6}$$

Similarly, if some force induces moment $\mathbf{M}_t$ directed along the tangent vector, the element gains the torsion

$$T = \|\mathbf{M}_t\| / \mathrm{GJ},$$

where GJ is a physical constant. In general, $\mathrm{GJ} \neq \mathrm{EI}$. The tangential vector $\mathbf{t}_0$, in this case, does not change the direction.

If the moment is given in an explicit form, then the resulting moment can be given as a sum of the explicit $\mathbf{M}_{\mathrm{ex}}$ and implicit $\mathbf{M}_F = \mathbf{r} \times \mathbf{F}$ moments:

$$\mathbf{M} = \mathbf{M}_{\mathrm{ex}} + \mathbf{M}_F . \tag{7}$$

2.2. Cross-section asymmetry. In general, an element may exhibit different rigidity in two planes (for example, a beam with the rectangular cross-section). To distinguish between the directions, introduce additional vectors $\boldsymbol{\xi}$ and $\boldsymbol{\eta}$ so that $\boldsymbol{\xi} \perp \boldsymbol{\eta}$. Together with $\mathbf{t}$, they form a right-handed triplet (Fig. 2). This implies the consideration of two bases having a common tangent vector, i.e.: $(\mathbf{t}, \boldsymbol{\xi}, \boldsymbol{\eta})$ is the "material" basis that is rigidly fixed and defines the reaction of an element to an external action as a physical solid, and $(\mathbf{t}, \mathbf{n}, \boldsymbol{\beta})$ is the "natural" one that rotates during the deformation indicating the direction of the resultant arc.

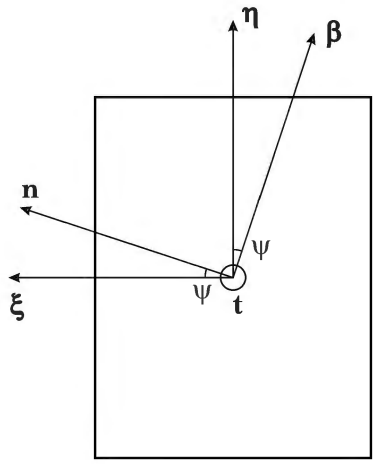

Fig. 2. The material and natural bases.

Introducing the material constants EI_ξ and EI_η, the non-tangential moment can be decomposed by two axes, as follows:

$$M_\xi = \mathrm{pr}(\mathbf{M}, \boldsymbol{\xi}), \quad M_\eta = \mathrm{pr}(\mathbf{M}, \boldsymbol{\eta}), \quad \mathbf{K} = \frac{M_\xi}{\mathrm{EI}_\xi}\boldsymbol{\xi} + \frac{M_\eta}{\mathrm{EI}_\eta}\boldsymbol{\eta}, \tag{8}$$

where $\mathrm{pr}(\mathbf{a}, \mathbf{b})$ denotes the projection of $\mathbf{a}$ onto $\mathbf{b}$.

2.3. Encountering for the initial curvature and torsion. Let an element has an initial curvature K_0 in the material direction $\boldsymbol{\eta}$. Then

$$\mathbf{K} = \frac{M_\xi}{\mathrm{EI}_\xi}\boldsymbol{\xi} + \left(K_0 + \frac{M_\eta}{\mathrm{EI}_\eta}\right)\boldsymbol{\eta}. \tag{9}$$

Defining the constituent of the moment that is directed alongside the tangential vector

$$M_t = \mathrm{pr}(\mathbf{M}, \mathbf{t}), \quad T = T_0 + M_t / \mathrm{GJ} \tag{10}$$

concludes the decomposition of the applied moment by the "material" basis:

$$\mathbf{M} = M_t \mathbf{t} + M_\xi \boldsymbol{\xi} + M_\eta \boldsymbol{\eta}. \tag{11}$$

Finally, making use of (6) and (8)–(11), we can establish the new scalar parameters for the natural basis, i.e.:

$$\mathbf{t}_0 = \text{const}, \quad \boldsymbol{\beta}_0 = \mathbf{K} / \mathrm{K}; \quad \mathbf{n}_0 = \boldsymbol{\beta}_0 \times \mathbf{t}_0. \tag{12}$$

2.4. Iterative process. When using TMM, all elements, except the first one, depend on the location and deformation of the previous element in the geometry. In order to reduce the input of this fact into the overall convergence, we use the approach of consequent computation, where the response of the ith element to the applied force is considered only after the response of the $(i+1)$th element is known. Then the conjugation conditions (1) are to be fulfilled by changing the location and the material basis of the current element so that they correspond to the ones located at the end of the previous one by using equations (5), i.e.:

$$\mathbf{p}_i(0) = \mathbf{p}_{i-1}(0) + \mathbf{AB}_{\mathbf{p}_{i-1}}(\ell_{i-1}) \begin{pmatrix} \mathbf{t}_{i-1}(0) \\ \mathbf{n}_{i-1}(0) \\ \boldsymbol{\beta}_{i-1}(0) \end{pmatrix},$$

$$\begin{pmatrix} \mathbf{t}_i(0) \\ \mathbf{n}_i(0) \\ \boldsymbol{\beta}_i(0) \end{pmatrix} = \mathbf{AB}_{\mathbf{t},\mathbf{n},\boldsymbol{\beta}_{i-1}}(\ell_{i-1}) \begin{pmatrix} \mathbf{t}_{i-1}(0) \\ \mathbf{n}_{i-1}(0) \\ \boldsymbol{\beta}_{i-1}(0) \end{pmatrix}. \tag{13}$$

When the new material basis of the element is known, we can decompose the applied moment (11) and calculate the new curvature, torsion, and natural basis (12).

It is possible to skip the moment application for some elements, while maintaining the continuity of the geometry. This would leave the natural basis unchanged, but will affect the angle ψ between the natural and material bases. In order to keep this angle correct, we can compute it for the not-yet-conjugated element, as follows:

$$\psi = \arccos\left(\mathbf{n}_0(0), \boldsymbol{\xi}_0(0)\right) \operatorname{sgn}\left(\arccos\left(\mathbf{n}_0(0), \boldsymbol{\eta}_0(0)\right) - \frac{\pi}{2} \right). \tag{14}$$

Then, after joining the element, the natural basis is to be corrected by rotating the material one about the axis $\mathbf{t}$, as follows:

$$\begin{pmatrix} \mathbf{n}_1(0) \\ \boldsymbol{\beta}_1(0) \end{pmatrix} = \begin{pmatrix} \cos\psi & -\sin\psi \\ \sin\psi & \cos\psi \end{pmatrix} \begin{pmatrix} \boldsymbol{\xi}_1(0) \\ \boldsymbol{\eta}_1(0) \end{pmatrix}. \tag{15}$$

In (14) and (15), the subscripts 0 and 1 denote the states before and after joining.

Each element is defined by 14 parameters (3) thus any geometry $\mathbf{G}$ consisting of N parameters can be treated as a $14 \times N$-dimensional vector. In the same way, the resulting moments from (7) form a $3 \times N$-dimensional vector $\mathbf{M}$. The foregoing procedures allow us to construct a subsequent geometry $\mathbf{G}_{n+1}$ based on a current geometry $\mathbf{G}_n$ and moments $\mathbf{M}_n$. Let us formalize this relation in the following way:

$$\mathbf{G}_{n+1} = \mathbf{g}(\mathbf{M}_n, \mathbf{G}_n), \tag{16}$$

Generally, there may be the case when moments themselves are not constant and depend on $\mathbf{G}$, itself. Let us denote this relation as $\mathbf{f}$, so that $\mathbf{M}_n = \mathbf{f}(\mathbf{G}_n)$. For example, the magnetic force varies with the distance between some points in geometry, inducing the change in the distance, itself. Thus, we can conclude the following: $\mathbf{M}_0 = \mathbf{f}(\mathbf{G}_0)$, $\mathbf{G}_1 = \mathbf{g}(\mathbf{M}_0, \mathbf{G}_0)$, then $\mathbf{M}_1 = \mathbf{f}(\mathbf{G}_1)$, $\mathbf{G}_2 = \mathbf{g}(\mathbf{M}_1, \mathbf{G}_1)$, etc. The goal for the routine (16) is the achievement of the final stable geometry $\mathbf{G}_{\text{fin}}$ and the corresponding moments $\mathbf{M}_{\text{fin}} = \mathbf{f}(\mathbf{G}_{\text{fin}})$, which meet the condition $\mathbf{g}(\mathbf{M}_{\text{fin}}, \mathbf{G}_{\text{fin}}) = \mathbf{G}_{\text{fin}}$.

It can be shown empirically that the Ibrahimbegovic problem [14] is instable which means that it is impossible to construct a convergent sequence (16). In order to improve the stability of the problem, we introduce the incremental algorithm with corresponding increment ratio $r_{\text{in}} \in (0,1]$ for computing the incremented moments as $\mathbf{I} = \mathbf{B} + (\mathbf{M} - \mathbf{B})r_{\text{in}}$. Ratio r_{in} can be made constant for all iterations. For example, if $r_{\text{in}} = 0.5$, then Bathe problem [2, 3] converges rapidly. However, it can be shown that for the Ibrahimbegovic problem the response varies depending on the current geometry. This narrows ratio r_{in} down to very low values, which increases the number of iterations. In order to improve the convergence, ratio r_{in} is to be increased from iteration to iteration for better convergence, or vice versa when the convergence is getting worse. For the formalization of this procedure, we present the list of all used metrics (as above, subscripts 0 and 1 correspond to the previous and current geometry):

1) $\Delta\boldsymbol{\theta}_{\max\angle} \stackrel{\text{def}}{=} \max\limits_i |\angle(\Delta\boldsymbol{\theta}_{i_0}, \Delta\boldsymbol{\theta}_{i_1})|$ presents the maximum increment of the bending angle;

2) $\Delta\boldsymbol{\theta}_{\text{mean}\angle} \stackrel{\text{def}}{=} \frac{1}{N}\sum\limits_i |\angle(\Delta\boldsymbol{\theta}_{i_0}, \Delta\boldsymbol{\theta}_{i_1})|$ presents the mean increment of the bending angle;

3) $T_{\max\Delta} \stackrel{\text{def}}{=} \max\limits_i |T_{i_0} - T_{i_1}|$ is the maximum increment of the torsion angle;

4) $T_{\text{mean}\Delta} \stackrel{\text{def}}{=} \frac{1}{N}\sum\limits_i |T_{i_0} - T_{i_1}|$ is the mean increment of the torsion angle;

5) $P_{\ell\Delta} \stackrel{\text{def}}{=} \frac{1}{\ell}\left\|\mathbf{P}(\ell)_{i_0} - \mathbf{P}(\ell)_{i_1}\right\|$ is the relative increment of the final point of the geometry.

Let us denote the set of these metrics as c_i. For each of them, we pick the corresponding threshold value c_i^* based on the empirical suggestions of the nature of the problem. Then we calculate the ultimate criterion $C = \max\limits_i C_i$, where $C_i = c_i / c_i^*$. If $C > 1$, then r_{in} is too large and should be decreased, e.g., by dividing r_{in} by C. Taking into consideration the error in performing operations with floating point, we recommend additional decrement of the computed coefficient by 1% in order to avoid possibility of getting into an endless cycle. By the same reason, if $\Delta\boldsymbol{\theta}_{i_0}$ and $\Delta\boldsymbol{\theta}_{i_1}$ are of the zero length, e.g., on the initial iteration, the angle between them is to be 0. If, otherwise, it equals π or $\pi/2$, then metrics *1*) or *2*) may not fall within the constrains despite ratio r_{in}. If $C < C_{\text{goal}} \ll 1$, then the current geometry is stable $\mathbf{G}_{\text{fin}}$, and thus the solution is attained.

Another problem which is observed when decreasing r_{in} is concerned with accident oscillations. This problem can be reduced by the following: for every final point of a geometry $\mathbf{P}_i(\ell)$, we compute

$$\mathbf{P}_{d,i} = \mathbf{P}_i(\ell) - \mathbf{P}_{i-1}(\ell), \quad P_\angle = \cos\angle(\mathbf{P}_{d,i}, \mathbf{P}_{d,i-1}),$$

$$C_{\cos} = \frac{P_\angle^2}{3} + \frac{\cos(P_\angle \pi/2)}{100}. \tag{17}$$

The ratio r_{in} is to be not greater than $P_{\angle}$. If the geometry is stable, then it can be shown that $r_{\text{in}} \to 1/3$ and $r_{\text{in}} \to 1/100$ otherwise. For the latter situation, we introduce the parameter

$$\mu = \begin{cases} 1.3, & P_{\angle} > 0.4, \\ 0.7, & |P_{\angle}| \le 0.4, \\ 0.5, & P_{\angle} < -0.4. \end{cases}$$

Then, the ratio can be computed as

$$r_{\text{in,corrected}} = \min\left(\min(r_{\text{in}}, P_{\angle})\mu, 1/3\right).$$

After implementing the foregoing steps, we can construct the solution using the following algorithm:

0. We begin with a geometry $\mathbf{G}_0$ consisting of N elements (in the general case – initially curved). We introduce the embedded moments $\mathbf{B}$, and since $\mathbf{G}_0$ does not undergo any load, $\mathbf{B}_0 = \mathbf{0}$.
1. At nth iteration, we have the embedded moments $\mathbf{B}_n$ and geometry $\mathbf{G}_n$, i.e., the basic curvature K, the basic torsion T, the directions of the tangent $\mathbf{t}_0$ and the (material) normal $\mathbf{n}_0$ at the starting point of each element, are known from the previous iteration.
2. We recompute the load values $\mathbf{M}_n = \mathbf{f}(\mathbf{G}_n) \neq \mathbf{B}_n$.
3. Taking (17) into account, we allow for an increment in moments, calculating $\mathbf{I}_n$.
4. For each element in $\mathbf{G}_n$ consecutively, we join it to the previous one, and then determine the new (refined) curvature, torsion and natural basis, using $\mathbf{I}_{n,i}$ as a moment vector.
5. For the newly formed geometry, we calculate metrics. If $C \ge 1$, geometry in question is discarded, ratio is decreased, and steps 3 and 4 are to be repeated.
6. If $C_{\text{goal}} < C < 1$, geometry is considered "threshold-compliant" and added to the sequence. The ratio is corrected. Execution continues from step 1.
7. If $C < C_{\text{goal}}$, geometry is adjusted to the applied forces and moments, and will not significantly change anymore. The solution is thereby found.

3. Numerical case studies.

3.1. Kirchhoff's problem. Kirchhoff showed [13] that a helix can be obtained from an initially straight rod by applying certain collinear torque $\mathbf{M}$ and force $\mathbf{F}$ (Fig. 3). We start with the following conditions: helix parameters are K and T, the number of winds is $N \in \mathbb{N}$, the initial rod has length ℓ and tangent $\mathbf{t}_0$. When $T = 0$ (the helix is a planar arc of circle), it is enough to calculate the "phase length" $\ell_{\varphi} \equiv 2\pi N$. In the general case, some part of the length ℓ corresponds to the movement in the direction perpendicular to the plane, so it turns out to be longer: $\ell = \ell_{\varphi}\sqrt{a^2 + h^2} \ge \ell_{\varphi}$, where a and h are given in (4).

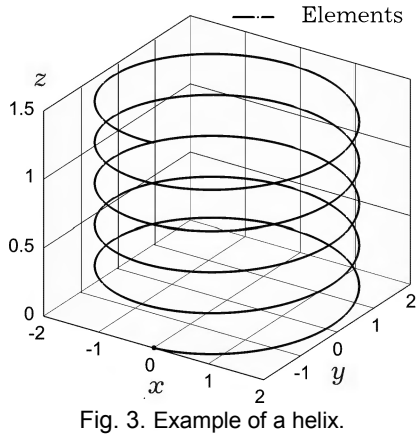

Fig. 3. Example of a helix.

In order to obtain a proper helix with a vertical axis, the starting line and, accordingly, the basis must be inclined, i.e.:

$$\mathbf{t}(s) = \frac{1}{\sqrt{a^2+h^2}}\begin{pmatrix} a \\ 0 \\ h \end{pmatrix}, \quad \boldsymbol{\xi}(s) = \begin{pmatrix} 0 \\ 1 \\ 0 \end{pmatrix}, \quad \boldsymbol{\eta}(s) = \mathbf{t}(s) \times \boldsymbol{\eta}(s), \quad \mathbf{p}(s) = s\mathbf{t}(s) - \begin{pmatrix} 0 \\ a \\ 0 \end{pmatrix}.$$

The physical constants EI and GJ are considered to be given.

According to Love's solution [13], the following torque and centered (at the point $\mathbf{F}_p = \mathbf{0}$) force should be applied:

$$\mathbf{M} = \frac{K^2\,\mathrm{EI} + T^2\mathrm{GJ}}{\sqrt{K^2+T^2}}\begin{pmatrix} 0 \\ 0 \\ 1 \end{pmatrix}, \quad \mathbf{F} = (\mathrm{GJ} - \mathrm{EI})\,T\sqrt{K^2+T^2}\begin{pmatrix} 0 \\ 0 \\ 1 \end{pmatrix}. \tag{18}$$

The latter force is to compensate the non-uniform torque when $\mathrm{GJ} \neq \mathrm{EI}$.

For each element, the procedure provides the same expression for the moment from the force:

$$\mathbf{M}_F = \mathbf{r} \times \mathbf{F} = a\,\|\mathbf{F}\|\,\mathrm{pr}(\mathbf{t}, xOy).$$

Since the arm of the force is collinear to the normal vector, which for the helix that complies with (18) lies in the horizontal plane, the moment from the force will also lie in this plane. As a result, we should get the desired helix:

$$\mathbf{p}(s) = \begin{pmatrix} a\sin\varphi \\ -a\cos\varphi \\ \varphi h \end{pmatrix}.$$

The projection of the total moment on the tangent is

$$\mathbf{M}_t = \frac{a\,\|\mathbf{M}_F\| + h\,\|\mathbf{M}_{ex}\|}{\sqrt{a^2+h^2}} = \frac{a^2\,\|\mathbf{F}\| + h\,\|\mathbf{M}\|}{\sqrt{a^2+h^2}}.$$

It can be verified analytically that, being divided by GJ, this value gives the desired T. Similarly, the curvature $\mathbf{K}$ is obtained correctly.

The proof-of-concept solution can be completed in one iteration if we artificially increase limits to accommodate the whole transformation. Thereby, $\Delta\boldsymbol{\theta}_{\max\angle}$ and $\Delta\boldsymbol{\theta}_{\mathrm{mean}\angle}$ could be zero because $\Delta\boldsymbol{\theta}$ is undefined (zero) for the initial geometry, and the angle between $\Delta\boldsymbol{\theta}_{i_0}$ and $\Delta\boldsymbol{\theta}_{i_1}$ is also zero. We can also compute

$$T_{\max\Delta} = T_{\mathrm{mean}\Delta} = \frac{1}{\mathrm{GJ}}\begin{pmatrix} a\,\|\mathbf{F}\| \\ 0 \\ \|\mathbf{M}\| \end{pmatrix} \cdot \mathbf{t}_0 = \frac{a^2\,\|\mathbf{F}\| + h\,\|\mathbf{M}\|}{\mathrm{GJ}\sqrt{a^2+h^2}},$$

$$P_{\ell\Delta} = \frac{a}{\sqrt{a^2+h^2}}.$$

We construct the helix with: $a = 2$, $h = 0.05$, $\mathrm{EI} = 1$, $\mathrm{GJ} = 0.8$, $N = 5$. Then $K = a/(a^2+h^2) \approx 0.4996877$ and $T = h/(a^2+h^2) \approx 0.01249219$. We start with a straight rod of length $\ell = 2\pi N\sqrt{a^2+h^2} \approx 62.85148496$ with

$$\mathbf{p}_0 = \begin{pmatrix} 0 \\ -a \\ 0 \end{pmatrix} = \begin{pmatrix} 0 \\ -2 \\ 0 \end{pmatrix}, \quad \mathbf{t}_0 = \frac{1}{\sqrt{a^2+h^2}}\begin{pmatrix} a \\ 0 \\ h \end{pmatrix} = \begin{pmatrix} 0.99968765 \\ 0 \\ 0.02499219 \end{pmatrix},$$

$$\boldsymbol{\xi}_0 = \begin{pmatrix} 0 \\ 1 \\ 0 \end{pmatrix}, \quad \boldsymbol{\eta}_0 = \mathbf{t}_0 \times \boldsymbol{\xi}_0 = \begin{pmatrix} -0.02499219 \\ 0 \\ 0.99968765 \end{pmatrix}.$$

According to (18), every element undergoes the upward moment with $\|\mathbf{M}\| \approx 0.49978138$ and the downward force with $\|\mathbf{F}\| \approx 0.00124883$. For the same reason as for the ratio, we slightly increase metric limits, i.e. $\Delta\theta_{\max\angle} = \Delta\theta_{\text{mean}\angle} = 0.001$, $T_{\max\Delta} = T_{\text{mean}\Delta} \approx 0.012505$, $P_{\ell\Delta} \approx 1.000687$. This allows us to achieve the correct solution after one iteration. For example, the total moment at the beginning of the beam is $\mathbf{M} \approx \begin{pmatrix} -0.00249766 \\ 0 \\ 0.49978138 \end{pmatrix}$. It can be shown that it complies with the decomposition procedure (11), (12):

$$\frac{1}{\mathrm{GJ}}\mathbf{M}\cdot\mathbf{t}_0 \approx 0.01249219 = T, \quad \mathbf{M}\cdot\boldsymbol{\xi}_0 = 0, \quad \frac{1}{\mathrm{EI}}\mathbf{M}\cdot\boldsymbol{\eta}_0 \approx 0.4996877 = K.$$

3.2. Bathe's problem [1]. Consider an initially curved beam lying in a plane and having a shape of an arc with central angle $\pi/4$ of a circle with $R=100$. It is assumed that force $\|\mathbf{F}\| = \lambda \mathrm{EI} / R^2 = \lambda 10^{-4}$, where λ is a scalar coefficient, is applied to the free end $\mathbf{p}_\ell$ of the beam in the upward direction, perpendicular to the plane (Fig. 4) and EI = GI = 1.

Initially,

$$\mathbf{p}_\ell = \begin{pmatrix} R(1-\cos\pi/4) \\ R\sin\pi/4 \\ 0 \end{pmatrix} \approx \begin{pmatrix} 29.289322 \\ 70.710678 \\ 0 \end{pmatrix}.$$

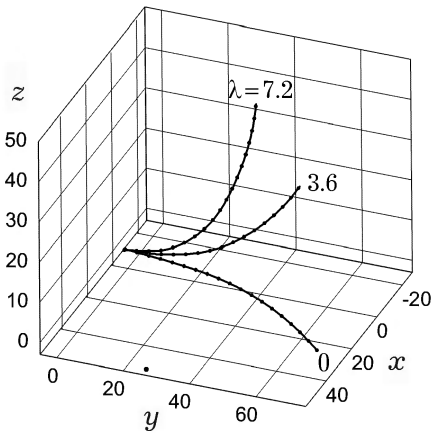

Fig. 4. Bathe's problem.

The numerical results are shown in the Tables 1 and 2, , where X, Y, and Z are components of the free end $\mathbf{p}_\ell$ of the beam.

Table 1. Bathe's problem with free end for $\lambda = 3.6$.

Variant		X	Y	Z
Our solution, number of elements	10	21.694592	57.461684	41.783721
	100	22.190905	58.644424	40.359238
	1000	22.23963	58.766126	40.205498
Albino et al. [2]		22.2	58.8	40.2
Bathe et al. [3]		22.5	59.2	39.5

Table 2. Bathe's problem with free end for $\lambda = 7.2$.

Variant		X	Y	Z
Our solution, number of elements	10	15.045353	45.243628	54.713814
	100	15.622659	46.95426	53.605801
	1000	15.678852	47.131527	53.48245
Albino et al. [2]		15.6	47.1	53.6
Bathe et al. [3]		15.9	47.2	53.4

3.3. Ibrahimbegovic's problem [14]. Consider an initially straight beam of length $\ell = 10$, $EI = GJ = 100$. Vertically upward torque $\|\mathbf{M}\| = 200\pi$ and force $\|\mathbf{F}\| = 50$ are applied to the free end of the beam. The "pseudo-time" parameter γ is introduced, which acts as a normalized (from 0 to 1) multiplier for $\mathbf{F}$ and $\mathbf{M}$. As in [14], an oscillation of the vertical movement of the last point is observed (Fig. 5). The numerical results are shown in Tables 3, 4 and 5.

Fig. 5. Free-end displacement component in the direction of applied force.

Table 3. Ibrahimbegovic's problem, beam end displacement, 10 elements.

γ, %	X	Y	Z
0	10.00000	0.000000	0.000000
3.6	3.892370	6.411033	-3.598481
9	-0.8338968	0.1693583	0.2668158
15	0.2997172	1.998785	-2.401981
25	0.1906868	1.154474	-2.779751
50	-0.05032712	0.04282715	-2.232799
100	1.816463×10^{-13}	-4.007788×10^{-14}	-1.584764×10^{-7}

Table 4. Ibrahimbegovic's problem, beam end displacement, 100 elements.

γ, %	X	Y	Z
0	10.00000	0.000000	0.000000
3.6	3.872713	6.544524	-3.309474
9	-0.5800782	0.09038742	1.201945
15	0.1021398	2.114726	-1.034295
25	0.05653336	1.268488	-0.8151035
50	-0.01211718	0.001188323	-0.3.646746
100	-0.02431667	0.005809512	-1.074613

Table 5. Ibrahimbegovic's problem, beam end displacement, 1000 elements.

γ, %	X	Y	Z
0	10.00000	0.000000	0.000000
3.6	3.869653	6.558041	-3.278281
9	-0.5556378	0.08878571	1.295173
15	0.07510166	2.119229	-0.8700036
25	0.02888077	1.272471	-0.5391933
50	0.01598553	2.761412×10^{-4}	0.1896195
100	0.001644169	-1.731448×10^{-5}	0.001689455

Conclusion. The methodology of basic and corrective solutions is generalized for the three-dimensional case. Solutions of simplified problems are considered, which, in fact, enable obtaining feasible result even without a corrective solution. Within the framework of the model, each TMM element is represented as a fragment of a helix line, that "accounts for" the corresponding values of the bending moment and axial force. The basic solution is the basis of the method, because it mainly takes the GN into account, and creates a system of coordinates and vectors, according to which the corrective (small geometrically linear) solution will be calculated in the future. Since obtaining a corrective solution for the three-dimensional case is quite a difficult task, this work focuses on the implementation of only the basic solution. Comparisons with known problems show that even a single basic method is sufficient to accurately approximate the solution with a small number of elements, usually orders of magnitude lower than required in linear models. Certain difficulties are observed when solving unstable problems, however, it is quite likely that they will be solved by the implementation of a corrective solution, as well as by improving the divergence detection algorithm.

1. *Ориняк І. В.* Розрахунки складних систем методом початкових параметрів. – Київ: Київ. політехн. ін-т ім. І. Сікорського, 2022. – 252 с. – https://ela.kpi.ua/handle/123456789/48744.
2. *Albino J. C. R., Almeida C. A., Menezes I. F. M., Paulino G. H.* Co-rotational 3D beam element for nonlinear dynamic analysis of risers manufactured with functionally graded materials (FGMs) // Eng. Struct. – 2018. – **173**. – P. 283–299. – http://doi.org/10.1016/j.engstruct.2018.05.092.
3. *Bathe K.-J., Bolourchi S.* Large displacement analysis of three-dimensional beam structures // Int. J. Numer. Meth. Eng. – 1979. – **14**, No. 7. – P. 961–986. – https://doi.org/10.1002/nme.1620140703.
4. *Bergou M., Wardetzky M., Robinson S., Audoly B., Grinspun E.* Discrete elastic rods // ACM Trans. Graph. (TOG). – 2008. – Article No. 63. – P. 1–12. – http://doi.org/10.1145/1399504.1360662.
5. *Connaire A., O'Brien P., Harte A., O'Connor A.* Advancements in subsea riser analysis using quasi-rotations and the Newton–Raphson method // Int. J. Non-Linear Mech. – 2015. – **70**. – P. 47–62. – https://doi.org/10.1016/j.ijnonlinmec.2014.10.021.
6. *Crisfield M. A.* A consistent co-rotational formulation for non-linear, three-dimensional, beam-elements // Comput. Methods Appl. Mech. Engng. – 1990. – **81**, No. 2. – P. 131–150. – https://doi.org/10.1016/0045-7825(90)90106-V.
7. *Crisfield M. A., Jelenić G.* Objectivity of strain measures in the geometrically exact three-dimensional beam theory and its finite-element implementation // Proc. Royal Soc. London A. – 1999. – **455**, No. 1983. – P. 1125–1147. – https://doi.org/10.1098/rspa.1999.0352.
8. *D'Amico B., Zhang H., Kermani A.* A finite-difference formulation of elastic rod for the design of actively bent structures // Eng. Struct. – 2016. – **117**. – P. 518–527. – https://doi.org/10.1016/j.engstruct.2016.03.034.
9. *Dittrich W.* The development of the action principle. A didactic history from Euler-Lagrange to Schwinger. – Cham: Springer, 2021. – xv + 135 p. – https://doi.org/10.1007/978-3-030-69105-9.
10. *Greco L., Cuomo M.* B-spline interpolation of Kirchhoff-Love space rods // Comput. Methods Appl. Mech. Engng. – 2013. – **256**. – P. 251–269. – https://doi.org/10.1016/j.cma.2012.11.017.
11. *Herath S., Yin G.* On the geometrically exact formulations of finite deformable isogeometric beams // Comput. Mech. – 2021. – **67**, No. 6. – P. 1705–1717. – https://doi.org/10.1007/s00466-021-02015-3.
12. *Koh S. K., Liu G.* Optimal plane beams modelling elastic linear objects // Robotica. – 2010. – **28**, No. 1. – P. 135–148. – https://doi.org/10.1017/S0263574709005669.
13. *Love A. E. H.* A treatise on the mathematical theory of elasticity. – Cambridge: Cambridge Univ. Press, 1920. – xviii + 624 p.
14. *Marino E.* Isogeometric collocation for three-dimensional geometrically exact shear-deformable beams // Comput. Methods Appl. Mech. Engng. – 2016. – **307**. – P. 383–410. – https://doi.org/10.1016/j.cma.2016.04.016.

15. *Mishani I., Sintov A.* Learning configurations of wires for real-time shape estimation and manipulation planning // Eng. Appl. Artif. Intel. – 2023. – **121**. – Article No. 105967. – https://doi.org/10.1016/j.engappai.2023.105967.
16. *Moll M., Kavraki L. E.* Path planning for deformable linear objects // IEEE T. Robot. – 2006. – **22**, No. 4. – P. 625–636. – https://doi.org/10.1109/TRO.2006.878933.
17. *O'Reilly O. M.* Modeling nonlinear problems in the mechanics of strings and rods. The role of the balance laws. – Cham: Springer, 2017. – xx + 425 p. – https://doi.org/10.1007/978-3-319-50598-5.
18. *Orynyak I., Guarracino F., Modano M., Mazuryk R.* An efficient iteration procedure for form finding of slack cables under concentrated forces // Arch. Civil Engng. – 2022. – **68**, No 2. – P. 645–663. – https://doi.org/10.24425/ace.2022.140664.
19. *Orynyak I., Mazuryk R.* Application of method of discontinuous basic and enhanced smoothing solutions for 3D multibranched cable // Engng Struct. B. – 2022. – **251**. – Article No. 113582. – https://doi.org/10.1016/j.engstruct.2021.113582.
20. *Orynyak I., Mazuryk R., Orynyak A.* Basic (discontinuous) and smoothing up (conjugated) solutions in transfer matrix method for static geometrically nonlinear beam and cable in plane // J. Eng. Mech. – 2020. – **146**, No. 5. – Article No. 04020031. – https://doi.org/10.1061/(ASCE)EM.1943-7889.0001753.
21. *Pai P. F., Anderson T. J., Wheater E. A.* Large-deformation tests and total-Lagrangian finite-element analyses of flexible beams // Int. J. Solids Struc. – 2000. – **37**, No. 21. – P. 2951–2980. – https://doi.org/10.1016/S0020-7683(99)00115-8.
22. *Rosen A., Gur O.* A transfer matrix model of large deformations of curved rods // Comp. Struct. – 2009. – **87**, Nos. 7-8. – P. 467–484. – https://doi.org/10.1016/j.compstruc.2008.12.014.
23. *Spillmann J., Teschner M.* Cosserat nets // IEEE T. Vis. Comp. Gr. – 2009. – **15**, No. 2. – P. 325–338. – https://doi.org/10.1109/TVCG.2008.102.
24. *Wakamatsu H., Hirai S.* Static modeling of linear object deformation based on differential geometry // Int. J. Robot. Res. – 2004. – **23**, No. 8. – P. 293–311. – https://doi.org/10.1177/0278364904041882.

3D АНАЛІЗ ГЕОМЕТРИЧНО НЕЛІНІЙНОГО ДЕФОРМУВАННЯ БАЛОК МЕТОДОМ БАЗОВИХ ГЕЛІКСНИХ ДІЛЯНОК

Розвинуто загальну методологію розв'язування геометрично нелінійних тривимірних задач деформування балок, основною складовою якої є базовий розв'язок у вигляді елемента гелікса. Досліджено основні параметри та властивості «малих» геліксних елементів та наведено методику їхнього ітеративного поєднання у великі тривимірні структури. Показано, що базовий розв'язок є самоузгодженим і може бути застосований лише для дослідження певних простих геометрій, наприклад, консольної балки. Проаналізовано відомі в літературі випадки, серед яких: а) задача Бате про початково плоску криволінійну балку, навантажену у вертикальному напрямку; б) задача Ібрагімбеґовича про початково пряму балку, навантажену вертикальним згинальним моментом і осьовою силою; в) задача Лява про створення гелікса з початково прямої гнучкої балки шляхом прикладання сили та моменту на її кінці.

Ключові слова: *деформація, тривимірні гнучкі балки, геометрична нелінійність, гелікс, метод початкових параметрів, метод базових і поправкових розв'язків.*

National Technical University of Ukraine
«Igor Sikorsky Kyiv Polytechnic Institute», Kyiv

Received
18.02.22